

Thermopower and Hall conductivity in the magnetic-field-driven normal state of $\text{Pr}_{2-x}\text{Ce}_x\text{CuO}_{4-\delta}$ superconductors

R. C. Budhani,* M. C. Sullivan, C. J. Lobb, and R. L. Greene

Center for Superconductivity Research, University of Maryland, College Park, Maryland 20742

(Received 9 October 2001; published 4 March 2002)

Measurements of thermoelectric power (TEP) and Hall coefficient (R_H) are carried out on $\text{Pr}_{2-x}\text{Ce}_x\text{CuO}_{4-\delta}$ epitaxial films to probe the mechanism of charge transport in the absence of superconductivity. In the underdoped ($x=0.13$) and optimally doped ($x=0.15$) samples, the TEP shows a $\ln(1/T)$ dependence and the R_H remains constant in the temperature range accessed by suppressing superconductivity. These observations and the behavior of the in-plane resistivity indicate weak localization of charge carriers on the CuO_2 planes. The TEP and R_H of the overdoped sample mimic metallic transport. This, combined with the evidence for hole and electron charge carriers, which may exist on different planes of the unit cell, suggests that the metallic transport in the overdoped samples is a consequence of a three-dimensional charge distribution.

DOI: 10.1103/PhysRevB.65.100517

PACS number(s): 74.25.Fy, 71.10.Hf, 74.72.Jt

The insulating behavior seen in the in-plane resistivity of the marginally doped, and in some cases optimally doped, cuprates in the presence of a magnetic field strong enough to quench superconductivity has remained an enigma.^{1–11} A $\ln(1/T)$ divergence of the resistivity and the assumption that the charge transport is confined to CuO_2 planes make two-dimensional (2D) weak localization^{12,13} a plausible mechanism for the metal-insulator (MI) transition. Indeed, the transverse negative magnetoresistance (MR) (Ref. 1) and the temperature-independent Hall coefficient (R_H) seen in some cases⁹ are consistent with the 2D weak-localization theory. Measurements of the c -axis and the ab -plane resistivity ρ_c and ρ_{ab} , respectively, in $\text{La}_{2-x}\text{Sr}_x\text{CuO}_4$ (LSCO) by Ando *et al.*¹ reveal that the ratio ρ_c/ρ_{ab} remains constant in the regime of temperature where $\rho_{ab} \sim \ln(1/T)$, suggesting the onset of a 3D behavior. These results make the 2D localization hypothesis less plausible. Anderson and co-workers⁴ have examined this issue in the 2D Luttinger liquid scenario where impurity disorder suppresses spin charge separation and leads to localization of the composite electrons. In this non-Fermi-liquid description of the ground state, the ρ_c/ρ_{ab} does not vary with temperature. The theory further predicts a temperature-independent Hall resistivity in the localization regime. Some recent theories⁹ and experimental works¹⁰ put the field-driven (FD) MI transition and the insulating behavior seen in the minimally doped nonsuperconducting compositions in the same universality class. Here the MI transition is driven by the localizing effects of the short-range antiferromagnetic correlations present in the system.⁸ Sekitani *et al.*¹¹ have argued that Kondo scattering of carriers by the uncompensated Cu^{2+} spins in the underdoped and optimally doped materials can also lead to the observed resistivity upturn and the negative MR. The isotropic negative MR seen in $\text{Nd}_{2-x}\text{Ce}_x\text{CuO}_4$ (NCCO) films¹¹ and $\text{La}_{2-x}\text{Sr}_x\text{CuO}_4$ (Refs. 14 and 15) lends support to this hypothesis. The other attempts to understand the FD-insulating state include impurity scattering in a marginal Fermi liquid⁵ and a bipolaron model⁶ for the condensate. The electron-electron (e - e) interaction effects in a 2D electronic system can also give rise to a $\ln(1/T)$ type of resistivity and a negative MR.¹⁵ It has also

been suggested² that a suppression of the density of states (DOS) at the Fermi energy (E_F) due to e - e interactions may lead to a constant ρ_c/ρ_{ab} .

Thus far, the experiments undertaken to distinguish between the various plausible mechanisms of the MI transition have been limited primarily to measurements of in-plane and c -axis resistivity, and the transverse magnetoresistance. Two important transport properties that can help resolve the competing theories for $\ln(1/T)$ behavior are the Hall coefficient and thermoelectric power (TEP). While the R_H has been measured in some cases,^{9,16} to the best of our knowledge there is no report of TEP measurements in the FD-normal state. Thermopower is a powerful probe of the charge-carrier scattering mechanisms, their spin state, and their energy distribution in the vicinity of the Fermi energy.^{17,18} Measurements of TEP can therefore provide valuable information about the origin of the FD-normal state in the cuprates.

In this paper we report measurements of temperature and magnetic-field-dependent TEP to address the origin of the field-driven MI transition in high- T_c cuprates. We have chosen $\text{Pr}_{2-x}\text{Ce}_x\text{CuO}_{4-\delta}$ epitaxial films with the doping level from underdoped to overdoped regimes. The choice of this system has been made because here the FD-normal state is easily accessible down to 1.2 K at relatively low fields (~ 10 T).³ These studies have been augmented by the measurements of R_H . We observe a qualitatively different temperature dependence of the TEP in samples which show insulating resistivity and those which do not. An increasing TEP and a constant R_H as the temperature is lowered in the FD-normal state of the underdoped and optimally doped samples suggest that the MI transition is driven by 2D weak localization of the charge carriers in the CuO_2 planes.

Epitaxial, c -axis oriented $\text{Pr}_{2-x}\text{Ce}_x\text{CuO}_{4-\delta}$ (PCCO) films of thickness 3000–3500 Å, and Ce concentration $x=0.13$ (underdoped), $x=0.15$ (optimally doped), and $x=0.17$ (overdoped), were deposited on (100) cut LaAlO_3 substrates using pulsed laser ablation.¹⁹ A standard eight-probe Hall bar geometry with the active film of $0.05 \times 1.0 \text{ cm}^2$ was used for measurements of ρ_{ab} , R_H , and TEP. For TEP measurements,

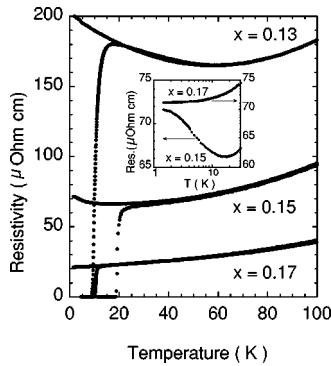


FIG. 1. The zero-field and in-field electrical resistivity of the underdoped ($x=0.13$), optimally doped ($x=0.15$), and overdoped ($x=0.17$) $\text{Pr}_{2-x}\text{Ce}_x\text{CuO}_{4-\delta}$ films plotted as a function of temperature. The strength of the magnetic field applied perpendicular to the plane of the film ($\parallel c$ axis) was 8.8 T for the optimally doped and 8.0 T for the other two films. Inset shows the resistivity of the overdoped and optimally doped films on a $\ln T$ scale.

one end of the sample was glued onto the copper cold finger of a vacuum probe, and the other end, left suspended, was heated to create a temperature gradient ∇T . Two miniature, magnetic-field-insensitive temperature sensors (CERNOX, from Lakeshore Cryotronics) allowed accurate measurement of the ∇T , which was kept below 7% of the absolute temperature. The TEP was measured against high-purity gold wires. The zero-field TEP of gold between 2.0 K and T_{co} , where T_{co} is the temperature at which a zero resistance state is reached in the films, was measured directly from the PCCO films. The absolute TEP of gold as a function of magnetic field at several temperatures was measured against an epitaxial film of $\text{YBa}_2\text{Cu}_3\text{O}_7$.

In Fig. 1 we show the in-plane resistivity of the three samples in a limited temperature range (1.5–100 K). One characteristic of the normal-state resistivity of these so-called electron doped superconductors is a quadratic T dependence of the normal-state resistivity. However, the $\rho \sim T^2$ dependence in the underdoped sample is truncated by the onset of an insulating behavior at lower temperatures. This leads to a minimum in $\rho_{ab}(T)$ at a characteristic temperature T^+ which increases with decreasing doping. The resistivity in the insulating region diverges as $\sim \ln(1/T)$. The underdoped sample becomes superconducting at still lower temperatures with a T_{co} of 9 K. The optimally doped sample reaches the zero resistance state at 19.9 K with a transition width ΔT of ~ 1 K. On increasing the Ce concentration to 0.17, the T_{co} drops to 9.8 K but the transition remains sharp ($\Delta T \sim 1$ K).

In Fig. 1 we also show the resistivity of these samples when a magnetic field strong enough to quench the superconductivity is applied. In the FD-normal state, the resistivity of the overdoped sample remains metallic, whereas for the underdoped and optimally doped samples a clear upturn in the resistivity is seen on lowering the temperature. An interesting feature of the resistivity in the FD-normal state is the devia-

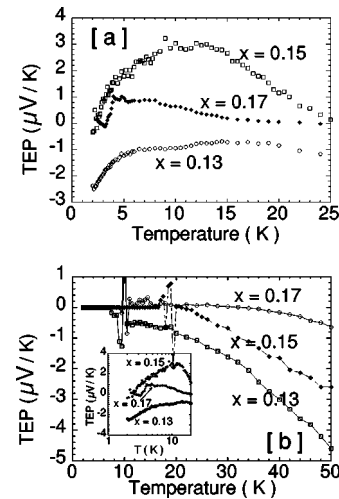


FIG. 2. (a) shows the TEP of the underdoped ($x=0.13$), optimally doped ($x=0.15$), and overdoped ($x=0.17$) films plotted as a function of temperature. These measurements were done in the field-driven normal state. The strength of the magnetic field applied perpendicular to the plane of the film ($\parallel c$ axis) was 8.8 T for the optimally doped and 8.0 T for the other two films. (b) shows the zero-field TEP of the same samples. The double peak structure in each curve marks the superconducting transition of the film. Inset of (b) shows the in-field data of (a) plotted on a $\ln T$ scale.

tion from a strict $\ln(1/T)$ divergence (see, inset Fig. 1). Fournier *et al.*²⁰ have attributed this effect to the saturation of the localization length.

Figure 2(a) shows the results of TEP measurements on the samples in their FD-normal state. For comparison, we have also shown the zero-field TEP of these samples in Fig. 2(b). These data are similar to earlier zero-field TEP measurements on NCCO films, of similar doping.^{20–23} We will, however, not dwell on the zero-field behavior, but highlight the fact that the TEP of the optimally doped and the underdoped samples is distinctly positive, albeit small, before the onset of the superconducting state. The TEP of the underdoped sample in the FD-normal state shows a $\ln(1/T)$ type of divergence down to the lowest temperature of measurement—a behavior similar to that of the resistivity. The TEP of the optimally doped sample is positive in the vicinity of the zero-field T_c . It decreases on cooling and seems to approach the $S=0$ line in the graph with a $\ln(1/T)$ dependence. This fact is highlighted in the inset of Fig. 2(b). For the overdoped sample, the TEP in the FD-normal state is very small, but distinctly positive, and it goes to zero within the accuracy of these measurements as the temperature goes to zero.

The thermopower due to charged quasiparticles is basically the entropy transported per unit charge. The TEP of a simple metal goes to zero linearly in temperature.²⁴ The contribution of uncharged excitations also goes to zero at $T=0$. When there is a clear gap in the density of states at E_F , the TEP at lower temperatures diverges as $1/T$.¹⁷ A scaling description of the thermopower in the elastic scattering limit for a 3D system near the mobility edge (E_c), as E_F

approaches E_c from the metallic side, shows that $S \sim 1/T$ if $k_B T \gg (E_F - E_c)$.²⁵ The corrections to TEP due to 2D weak localization have also been worked out. While an early study²⁶ showed that the quantum interference affects conductivity (σ) and thermoelectric coefficient (η) identically, leading to no change in $S (= \sigma/\eta)$, the later works^{27–29} suggest a $\ln(1/T)$ divergence of the TEP as well. While this conclusion has also been questioned,³⁰ our TEP data for the underdoped and optimally doped samples seem to suggest a $\ln(1/T)$ dependence. A full confirmation of this would, however, require measurements at still lower temperatures, which are certainly nontrivial given that the TEP of these samples is quite small. It is also of interest to see how the TEP in the FD-normal state depends on the orientation of the magnetic field with respect to the CuO_2 planes and the direction of ∇T . This will help understand whether the $\ln(1/T)$ dependence is truly an orbital effect or not. Presently, this is complicated by the fact that the magnetic field used in this study barely exceeds the H_{c2} for $H \parallel c$ -axis configuration. The upper critical field for $H \parallel ab$ plane is much higher for these superconductors. However, measurements of transverse and longitudinal magnetoresistance in underdoped (nonsuperconducting) films of PCCO (Ref. 20) clearly show that the negative magnetoresistance is an orbital effect, consistent with 2D weak localization.

At this stage it is important to consider how the e - e interactions in a 2D disordered system would affect the TEP. While this picture predicts a logarithmic correction to TEP,²⁶ its value at $T=0$ goes to zero, just as in the case of a metal. One important consequence of the e - e interactions is a reduction in the density of states at the Fermi energy, some signatures of which are seen in the tunneling data on PCCO.³¹ In the presence of strong disorder, there is a likelihood that an Efros-Shklovskii-type Coulomb gap³² opens up at the E_F . Burns and Chaikin³³ have shown that, in such a case, the TEP should increase with decreasing T and level off to a nonzero value at $T=0$. However, such strong localization is possible only when $k_F l < 1$, where k_F is the Fermi wave vector and l the electronic mean free path. Since the $k_F l$ parameter for our optimally doped and underdoped samples is much larger than 1, we do not expect an Efros-Shklovskii-type gap at E_F in the present case.

A further support to the localization picture for the FD-normal state comes from the measurements of R_H . While the theory of weak localization predicts no change in R_H ,¹¹ the e - e interactions cause a correction to R_H , which is twice as big as the correction to resistance.¹⁵ In the non-Fermi-liquid description of the 2D weak localization and transport,⁴ the Hall resistivity (ρ_{xy}) is expected to reach a constant value at low temperatures. In Fig. 3 we show the variation of R_H as a function of $\ln(T)$ for the three samples. For the underdoped and optimally doped samples, the R_H becomes temperature independent below ~ 15 and 9 K, respectively. This observation is consistent with the predictions of the theory of localization in 2D Luttinger liquids. Here it needs to be stated that a similar behavior of R_H in the FD-normal state has been

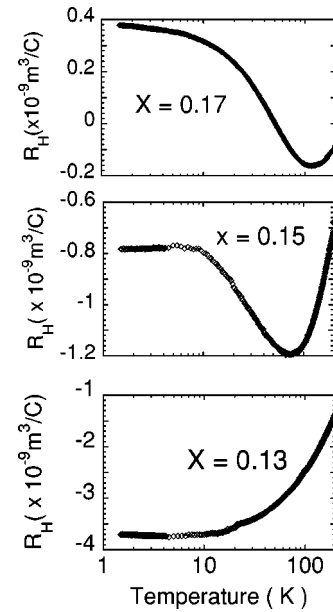


FIG. 3. Temperature dependence of the R_H of the overdoped, optimally doped, and underdoped films is shown in the top, middle, and bottom panels respectively. Note that the x axis is in logarithmic scale. The R_H has been calculated from the measurements of ρ_{xy} vs T at 8.0 T for $x=0.13$ and $x=0.17$ samples, and at 8.8 T for the optimally doped sample.

seen in $\text{La}_{2-x}\text{Sr}_x\text{CuO}_4$.⁹ However, a constant R_H is seen even in the overdoped sample of $x=0.23$ where the FD-normal state is metallic.

The R_H of the overdoped sample undergoes a sign change from negative to positive value at $T=60$ K. Below 9 K, it increases monotonically with decreasing temperature down to the lowest temperature of measurement. A temperature dependent R_H and a metallic resistivity in the FD-normal state has also been seen in the hole doped, single layer cuprate $\text{Tl}_2\text{Ba}_2\text{CuO}_{6+\delta}$.¹⁶ Interestingly, the zero-field resistivity of this system is also quadratic in temperature as in the case of the electron doped superconductor. The sign reversal and a strong temperature dependence of R_H in electron doped cuprates has been seen as an indication of two bands with oppositely charged current carriers.^{21–23,34} Our measurements of flux flow thermopower³⁵ provides further evidence for two types of carriers in these systems at high doping levels. At present it is not clear where the p -type carriers reside given that substitution of Ce at Pr sites leads to electron doping of the CuO_2 planes. Geballe and Mayzhes³⁶ have argued that the mobile electrons and holes exist in the CuO_2 planes and oxygen planes, respectively, of the T^* structure of these compounds. This type of charge distribution will certainly make the unit cell electronically three-dimensional and thus reduce the tendency towards 2D localization. As we move towards the underdoped compositions, the number density of holes goes down, and the electrons in the CuO_2 planes become prone to 2D localization by the impurity and spin correlation disorders. Since the resistivity ratio (ρ_c/ρ_{ab}), where ρ_c and ρ_{ab} are c -axis and ab -plane resistivity, respectively, in hole doped systems decreases rapidly with doping,³⁷ we further argue that our picture of increasing

dimensionality on the overdoped side and a 2D charged liquid (perhaps unconventional) subjected to spin and impurity disorder on the underdoped side, can be extended to the hole doped cuprates as well.

In summary, we have reported systematic measurements of thermopower in the field-driven normal state of overdoped, optimally doped, and underdoped $\text{Pr}_{2-x}\text{Ce}_x\text{CuO}_{4-\delta}$. These measurements augmented by the measurements of R_H and resistivity support the idea that the

magnetic field driven MI transition in the cuprates is caused by 2D weak localization.

We thank Vera Smolyaninova, Amlan Biswas, and Joshua Higgins for useful comments during the course of these measurements, and Bin Ming for providing the YBCO film. This work has been supported by the NSF under Grant No. DMR-0102350.

*On leave from the Department of Physics, Indian Institute of Technology Kanpur, Kanpur-208016, India.

¹Y. Ando *et al.*, Phys. Rev. Lett. **75**, 4662 (1995).

²G. S. Boebinger *et al.*, Phys. Rev. Lett. **77**, 5417 (1996).

³P. Fournier *et al.*, Phys. Rev. Lett. **81**, 4720 (1998).

⁴P. W. Anderson *et al.*, Phys. Rev. Lett. **77**, 4241 (1996).

⁵C. M. Varma, Phys. Rev. Lett. **79**, 1535 (1997).

⁶A. S. Alexandrov *et al.*, Phys. Rev. Lett. **77**, 4796 (1996).

⁷P. A. Marchetti *et al.*, Phys. Rev. Lett. **86**, 3831 (2001).

⁸V. J. Emery *et al.*, Phys. Rev. B **56**, 6120 (1997).

⁹Y. Ando *et al.*, Phys. Rev. B **56**, R8530 (1997).

¹⁰Y. Ando *et al.*, Phys. Rev. Lett. **87**, 017001 (2001).

¹¹T. Sekitani *et al.*, Physica B **294**, 358 (2001).

¹²E. Abrahams *et al.*, Phys. Rev. Lett. **42**, 673 (1979).

¹³N. W. Preyer *et al.*, Phys. Rev. B **44**, 407 (1991).

¹⁴Z. A. Xu *et al.*, Physica C **341–348**, 1711 (2000).

¹⁵B. L. Altshuler and A. G. Aronov, in *Electron-Electron Interactions in Disordered Systems*, edited by M. Pollak and A. L. Efros (North-Holland, Amsterdam, 1985), pp. 1-153.

¹⁶A. P. Mackenzie *et al.*, Phys. Rev. B **53**, 5848 (1996).

¹⁷P. M. Chaikin, in *Organic Superconductors*, edited by V. Z. Kresin and W. A. Little (Plenum, New York, 1990), pp. 101–115.

¹⁸Wu Jiang *et al.*, Phys. Rev. B **48**, 657 (1993).

¹⁹E. Maiser *et al.*, Physica C **297**, 15 (1998).

²⁰P. Fournier *et al.*, Phys. Rev. B **62**, R11 993 (2000).

²¹P. Fournier *et al.*, Phys. Rev. B **56**, 14 149 (1997).

²²Wu Jiang *et al.*, Phys. Rev. Lett. **73**, 1291 (1994).

²³F. Gollnik and M. Naito, Phys. Rev. B **58**, 11 734 (1998).

²⁴F. J. Blatt, P. A. Schroeder, C. L. Foiles, and D. Greig, *Thermoelectric Power of Metals* (Plenum, New York, 1976).

²⁵U. Sivan and Y. Emry, Phys. Rev. B **33**, 551 (1986).

²⁶C. S. Ting *et al.*, Phys. Rev. B **25**, 1439 (1982).

²⁷V. V. Afonin *et al.*, Phys. Rev. B **33**, 8841 (1986).

²⁸C. Castellani *et al.*, Phys. Rev. B **37**, 6663 (1988).

²⁹M. J. Kearney *et al.*, Phys. Rev. Lett. **66**, 1622 (1991).

³⁰J. E. Enderby and A. C. Barnes, Phys. Rev. B **49**, 5062 (1994).

³¹A. Biswas *et al.*, Phys. Rev. B **64**, 104519 (2001).

³²A. L. Efros and B. I. Shklovskii, in *Electron-Electron Interactions in Disordered Systems*, edited by M. Pollak and A. L. Efros (North-Holland, Amsterdam, 1985), pp. 409–482.

³³M. J. Burns and P. M. Chaikin, J. Phys. C **18**, L743 (1985).

³⁴Z. Z. Wang *et al.*, Phys. Rev. B **43**, 3020 (1991).

³⁵R. C. Budhani *et al.* (unpublished).

³⁶T. H. Gaballe and B. Y. Mozyhes (unpublished).

³⁷T. Ito *et al.*, Nature (London) **350**, 596 (1991).